

Mathematical and Physical Properties of Three-Band  $s_{\pm}$  Eliashberg Theory for Iron Pnictides

*Original*

Mathematical and Physical Properties of Three-Band  $s_{\pm}$  Eliashberg Theory for Iron Pnictides / Ummarino, Giovanni. - In: MAGNETOCHEMISTRY. - ISSN 2312-7481. - ELETTRONICO. - 9:1(2023), p. 28. [10.3390/magnetochemistry9010028]

*Availability:*

This version is available at: 11583/2974521 since: 2023-01-11T16:19:25Z

*Publisher:*

MDPI

*Published*

DOI:10.3390/magnetochemistry9010028

*Terms of use:*

This article is made available under terms and conditions as specified in the corresponding bibliographic description in the repository

*Publisher copyright*

(Article begins on next page)



## Article

# Mathematical and Physical Properties of Three-Band $s\pm$ Eliashberg Theory for Iron Pnictides

Giovanni Alberto Ummarino <sup>1,2</sup>

- <sup>1</sup> Istituto di Ingegneria e Fisica dei Materiali, Dipartimento di Scienza Applicata e Tecnologia, Politecnico di Torino, Corso Duca degli Abruzzi 24, 10129 Torino, Italy; giovanni.ummarino@polito.it
- <sup>2</sup> Moscow Engineering Physics Institute, National Research Nuclear University MEPhI, Kashirskoe Shosse 31, 115409 Moscow, Russia

**Abstract:** The phenomenology of the iron pnictide superconductor can be described by the three-band  $s\pm$  Eliashberg theory in which the mechanism of superconducting coupling is mediated by antiferromagnetic spin fluctuations and whose characteristic energy  $\Omega_0$  scales with  $T_c$  according to the empirical law  $\Omega_0 = 4.65k_B T_c$ . This model presents the universal characteristics that are independent of the critical temperature, such as the link between the two free parameters  $\lambda_{13}$  and  $\lambda_{23}$  and the ratio  $\Delta_i/k_B T_c$ .

**Keywords:** antiferromagnetic spin fluctuations; superconducting materials; Fe-based superconductors; multiband Eliashberg theory



**Citation:** Ummarino, G.A. Mathematical and Physical Properties of Three-Band  $s\pm$  Eliashberg Theory for Iron Pnictides. *Magnetochemistry* **2023**, *9*, 28. <https://doi.org/10.3390/magnetochemistry9010028>

Academic Editor: Evgeny Katz

Received: 30 November 2022

Revised: 4 January 2023

Accepted: 9 January 2023

Published: 11 January 2023



**Copyright:** © 2023 by the author. Licensee MDPI, Basel, Switzerland. This article is an open access article distributed under the terms and conditions of the Creative Commons Attribution (CC BY) license (<https://creativecommons.org/licenses/by/4.0/>).

## 1. Introduction

The superconductive compounds based on iron and arsenic have been discovered for more than fifteen years, and all experimental data have been successfully reproduced using the multiband Eliashberg theory. The mechanism responsible for the pairing is mainly due to antiferromagnetic spin fluctuations. The various compounds can be described mainly by three- [1–5], four- [6] or five- [7] band models, while the two-band model is purely phenomenological, and, in this case, the values of the electron–boson coupling constants have no physical significance. In most cases, the three-band model is sufficient to describe the experimental data relating to these materials. Therefore, we will consider the properties of a three-band model in which a fundamental role will be played by the assumption that the representative energy of these systems  $\Omega_0$  is related to the critical temperature by a universal linear relationship [8,9]  $\Omega_0 = 4.65k_B T_c$ , and the symmetry of the order parameter is  $s\pm$  [10–12]. In the past, J.M. Coombes and J.P. Carbotte [13–15] found that, if all of the energy scales of the electron–phonon spectral function, in the single band s-wave Eliashberg equations shrink or expand, the rate between the gap and the critical temperature does not change. This result is exact if the Coulomb pseudopotential is zero. When examining the Eliashberg equations for a multiband system, it is possible to see that this scaling theorem continues to hold, and the values of the gaps and of the critical temperature have increased or decreased by the same factor with which the energy scale has increased or decreased. In fact, Eliashberg’s equations for a multiband system are the sum of individual pieces where, in each of which, we can expand or restrict the energy scale. Additionally, in this case, the result is correct only if all values of the Coulomb pseudopotential are zero. The novelty of our work is, essentially, that it sheds light on the universal bond that exists between the coupling constants as they relate to the single band.

## 2. The Model

The simplest model to describe the phenomenology of iron pnictides within Eliashberg’s theory consists of a three-band  $s\pm$  model with two holonic and one electronic. In this

way, the two gaps of the hole bands,  $\Delta_1$  and  $\Delta_2$ , have an opposite sign from the gap residing on the electron band, i.e.,  $\Delta_3$ . The interband coupling between the hole and electron bands is mainly provided by antiferromagnetic spin fluctuations (*sf*), while phonons can be responsible for the intraband coupling (*ph*) [10]. The antiferromagnetic spin fluctuation coupling between bands with the same type of charge carriers (holes with holes and electrons with electrons) is zero, while the total phonon coupling is very small ( $<0.35$ ) [16]. We assume that the symmetry of this system is  $s\pm$ , and the electron–boson coupling is from antiferromagnetic spin fluctuations and, in very small part, from phonons. The interband coupling constants in this paper are just relative to the antiferromagnetic spin fluctuations and are positive because we, as usual, change the sign inside the equations. To calculate the gaps and the critical temperature, we use the three-band  $s\pm$  wave Eliashberg equations with infinite bandwidth [17–20]. The infinite bandwidth approximation is always applicable in iron pnictides. Eliashberg’s equations, without this approximation, are more complicated [21,22], and the solutions diverge appreciably only in striking cases, such as, for example, in strontium titanate (SrTiO) [23]. In the case of one-band systems, the same results are obtained except in extreme cases in which the width of the conduction band is comparable to the phonon energies [24]. We have to solve six coupled equations: three for the gaps  $\Delta_i(i\omega_n)$  and three for the renormalization functions  $Z_i(i\omega_n)$ , in which  $i$  is a band index (that ranges between one and three), and  $\omega_n$  are the Matsubara frequencies. The imaginary axis equations [25–27], when the Migdal theorem [28] is valid, read as follows:

$$\omega_n Z_i(i\omega_n) = \omega_n + \pi T \sum_{m,j} \Lambda_{ij}^Z(i\omega_n, i\omega_m) N_j^Z(i\omega_m) + \sum_j [\Gamma_{ij}^N + \Gamma_{ij}^M] N_j^Z(i\omega_n) \quad (1)$$

$$Z_i(i\omega_n) \Delta_i(i\omega_n) = \pi T \sum_{m,j} [\Lambda_{ij}^\Delta(i\omega_n, i\omega_m) - \mu_{ij}^*(\omega_c)] \times \Theta(\omega_c - |\omega_m|) N_j^\Delta(i\omega_m) + \sum_j [\Gamma_{ij}^N - \Gamma_{ij}^M] N_j^\Delta(i\omega_n) \quad (2)$$

where  $\Gamma_{ij}^N$  and  $\Gamma_{ij}^M$  are the scattering rates from the non-magnetic and magnetic impurities,  $\Lambda_{ij}^Z(i\omega_n, i\omega_m) = \Lambda_{ij}^{ph}(i\omega_n, i\omega_m) + \Lambda_{ij}^{sf}(i\omega_n, i\omega_m)$  and  $\Lambda_{ij}^\Delta(i\omega_n, i\omega_m) = \Lambda_{ij}^{ph}(i\omega_n, i\omega_m) - \Lambda_{ij}^{sf}(i\omega_n, i\omega_m)$  for which

$$\Lambda_{ij}^{ph,sf}(i\omega_n, i\omega_m) = 2 \int_0^{+\infty} d\Omega \Omega \alpha_{ij}^2 F^{ph,sf}(\Omega) / [(\omega_n - \omega_m)^2 + \Omega^2].$$

where  $\Theta$  is the Heaviside function, and  $\omega_c$  is a cutoff energy. The quantities  $\mu_{ij}^*(\omega_c)$  are the elements of the  $3 \times 3$  Coulomb pseudopotential matrix. Finally,  $N_j^\Delta(i\omega_m) = \Delta_j(i\omega_m) / \sqrt{\omega_m^2 + \Delta_j^2(i\omega_m)}$ , and  $N_j^Z(i\omega_m) = \omega_m / \sqrt{\omega_m^2 + \Delta_j^2(i\omega_m)}$ . The electron–boson coupling constants are defined as  $\lambda_{ij}^{ph,sf} = 2 \int_0^{+\infty} d\Omega \frac{\alpha_{ij}^2 F^{ph,sf}(\Omega)}{\Omega}$ .

To solve Equations (1) and (2), it is first necessary to specify a certain number of input parameters, which depends on particular characteristics of the studied system. Often, it is possible through drastic approximations to reduce the number of input parameters, which are not always known, without renunciation to accurately describe the physics of the system. In the case of a three-band model, we have nine electron–phonon spectral functions  $\alpha_{ij}^2 F^{ph}(\Omega)$ , nine electron–antiferromagnetic spin fluctuation spectral functions,  $\alpha_{ij}^2 F^{sf}(\Omega)$ , nine elements of the Coulomb pseudopotential matrix  $\mu_{ij}^*(\omega_c)$ , and nine nonmagnetic  $\Gamma_{ij}^N$  and nine paramagnetic  $\Gamma_{ij}^M = 0$  impurity-scattering rates. Luckily, a lot of these parameters can be extracted from experiments, and some can be fixed by suitable approximations. In

fact, fortunately, the system that we want to describe, the iron pnictides, has particular characteristics that allow numerous strong approximations aimed at reducing the number of free parameters. Despite this, the model still allows the main properties of these materials to be described in an extremely precise way. In particular, we refer to experimental data taken on high-quality samples, so we can rather safely assume a negligible disorder and put the scattering from the non-magnetic and magnetic impurities  $\Gamma_{ij}^{N,M}$  equal to zero. We know that in these materials the total electron–phonon coupling constant is small (the upper limit of these compounds is  $\approx 0.35$  [16]), and the phonons mainly provide *intraband* coupling so that  $\lambda_{ij}^{ph} \approx 0$  [10]. Furthermore, it is well-established that the superconducting glues are provided by antiferromagnetic spin fluctuations. These last bosons mainly provide [10] interband coupling between holes and electron bands, so that  $\lambda_{12}^{sf} = \lambda_{21}^{sf} = \lambda_{ii}^{sf} = 0$ . To reduce the number of free parameters without altering the physics of the system, we set, in the first approximation, the phonon intraband coupling equal to 0.1 so that  $\lambda_{ii}^{ph} = 0.1$ , and the Coulomb pseudopotential matrix [12,25–27]  $\mu_{ii}^*(\omega_c) = \mu_{ij}^*(\omega_c) = 0$ . As we discussed before, the maximum value of the total electron–phonon coupling is estimated at less than 0.35, which is a bit larger than the Coulomb pseudopotential that has the opposite sign, so, in the first approximation, and to reduce the number of free parameters, we set the pseudopotential equal to zero, and the intraband phonon coupling equal to 0.1 because the second reduces the first. Of course, this does not mean that the phonons are absent—just that the final result in the calculus of a lot of physical properties is not influenced by their presence. Within these approximations, the electron–boson coupling constant matrix  $\lambda_{ij}$  becomes [25–27]:

$$\lambda_{ij} = \begin{pmatrix} 0.1 & 0 & \lambda_{13}^{sf} \\ 0 & 0.1 & \lambda_{23}^{sf} \\ \lambda_{31}^{sf} = \lambda_{13}^{sf} \nu_{13} & \lambda_{32}^{sf} = \lambda_{23}^{sf} \nu_{23} & 0.1 \end{pmatrix} \quad (3)$$

where  $\nu_{ij} = N_i(0)/N_j(0)$ , and  $N_i(0)$  is the normal density of the states at the Fermi level for the  $i$ -th band. The coupling constants  $\lambda_{ij}^{sf}$  are defined through the electron–antiferromagnetic spin fluctuation spectral functions (Eliashberg functions)  $\alpha_{ij}^2 F_{ij}^{sf}(\Omega)$ . We chose for these functions to have a Lorentzian shape [25–27], which reproduces the experimentally measured form quite well [29]:

$$\alpha_{ij}^2 F_{ij}^{sf}(\Omega) = C_{ij} \{ L(\Omega + \Omega_{ij}, Y_{ij}) - L(\Omega - \Omega_{ij}, Y_{ij}) \}, \quad (4)$$

where

$$L(\Omega \pm \Omega_{ij}, Y_{ij}) = \frac{1}{(\Omega \pm \Omega_{ij})^2 + Y_{ij}^2}$$

and  $C_{ij}$  are the normalization constants necessary to obtain the proper values of  $\lambda_{ij}$ , while  $\Omega_{ij}$  and  $Y_{ij}$  are the peak energies and the half-widths of the Lorentzian functions, respectively [27]. In all calculations, we set  $\Omega_{ij} = \Omega_0$ , i.e., we assume that the characteristic energy of antiferromagnetic spin fluctuations is a single quantity for all of the coupling channels and that  $Y_{ij} = \Omega_0/2$ , based on the results of inelastic neutron scattering measurements [29].

The peak energy of the Eliashberg functions,  $\Omega_0$ , can be directly associated with the experimental critical temperature,  $T_c$ , by using the empirical law  $\Omega_0 = 4.65 k_B T_c$ , which has been demonstrated to hold, at least approximately, for iron pnictides [8,9]. With all of these approximations, which are necessary to reduce the number of free parameters, this is the simplest model that can still grasp the essential physics of iron compounds. The cutoff energy is  $\omega_c = 6.7568 \Omega_0$ . We assume, just for simplicity, that the electron–phonon spectral functions have the same shape as the electron–antiferromagnetic spin fluctuation spectral functions.

The factors  $\nu_{ij} = \frac{N_i(0)}{N_j(0)}$  that enter the definition of  $\lambda_{ij}$  (Equation (3)) are free parameters, so we examine five different exhaustive situations: the first case is  $\nu_{13} = 0.2$  and  $\nu_{23} = 1$ ;

the second case is  $\nu_{13} = 0.5$  and  $\nu_{23} = 1$ ; the third case is  $\nu_{13} = 1$  and  $\nu_{23} = 1$ ; the fourth case is  $\nu_{13} = 2$  and  $\nu_{23} = 1$ ; and the fifth case is  $\nu_{13} = 5$  and  $\nu_{23} = 1$ . At the end, we fixed the  $N_i(0)$  for each case; we have just two free parameters  $\lambda_{13}$  and  $\lambda_{23}$ , so we change  $\lambda_{13}$ , and we fix  $\lambda_{23}$  in order to obtain the correct critical temperature. In the known multiband superconductors and, specifically, in the iron pnictides, the values of the densities of the states at the Fermi level  $N_i(0)$  relating to the various bands are roughly of the same order of magnitude. Therefore, in the five cases examined, we have exhausted all of the possible cases that have occurred to date. In principle, it is easy to calculate the densities of the states at the Fermi level for the bands of a given material, while it is much more complicated to calculate the electron–boson coupling constants, especially when the mechanism is the antiferromagnetic spin fluctuations. It is possible to define a total electron boson coupling constant (with sign)  $\lambda_{tot} = \sum_{i,j=1}^2 N_i(0)\lambda_{ij} / \sum_{i=1}^2 N_i(0)$  where the coupling constant related to antiferromagnetic spin fluctuations are negative.

### 3. Discussion

In Figures 1 and 2, it is possible to see  $|\lambda_{23}|$  ( $\lambda_{tot}$ ) as a function of  $|\lambda_{13}|$  in the various cases examined. The relevant thing is that these curves are universal; they are valid for any critical temperature. In Figure 1, it is possible to see that all curves pass through the point  $|\lambda_{13}| = 0.95$  and  $|\lambda_{23}| = 2.37$ . With the same values of  $|\lambda_{13}|$  and  $|\lambda_{13}| = 0.953$ , what changes is only the total value of the electron–boson coupling. Then, in the particular case in which  $|\lambda_{13}| = 0.95$  and  $|\lambda_{23}| = 2.37$ , the variation range of the total electron–boson coupling is:  $-2.2 < \lambda_{tot} < -1.9$ . The universality derives from the fact that we impose a very strong (experimental) constraint on the energy of the peak of the spectral functions  $\Omega_0 = 4.65k_B T_c$ . The universality of Figures 1 and 2 lies in the fact that, once the densities of the states at the Fermi level  $N_i(0)$  relating to the single bands have been fixed, there is an unequivocal relationship between the two coupling constants  $\lambda_{13}$  and  $\lambda_{23}$ : once one is fixed, there can exist only one value of the other that reproduces the correct  $T_c$ . From these curves, it is also possible to see that  $0 < |\lambda_{23}| < 3.5$ , and  $0 < |\lambda_{13}| < 7.5$ . Additionally, this result does not depend on the particular critical temperature  $1.1 < |\lambda_{tot}| < 2.3$ . This means that, in principle, for all iron pnictides, the total coupling is, in absolute value, less than 2.3, and this fact means that they can be just in a state of moderate strong coupling. In Figure 3, the  $|\Delta_i|/k_B T_c$  ratios are shown for the three gaps with three different critical temperatures ( $T_c = 37$  K,  $T_c = 57$  K and  $T_c = 200$  K), and, as you can see, the results are perfectly superimposable. Here, of course,  $|\Delta_i|$  is calculated from the solution to the Eliashberg equations, at  $T \ll T_c$ , by using Padé approximants. The same happens also for the superconducting densities of states, as it is possible to see in Figure 4. The superconducting densities of states, calculated at  $T = T_c/12$ , for  $T_c = 37$  K,  $T_c = 57$  K and  $T_c = 200$  K versus  $\omega/\Omega_0$  in the first ( $\nu_{13} = 0.2$  and  $\nu_{23} = 1$  with  $\lambda_{13} = 6.0000$  and  $\lambda_{23} = 1.1577$ ) and third cases ( $\nu_{13} = 1$  and  $\nu_{23} = 1$  with  $\lambda_{13} = 0.95$  and  $\lambda_{23} = 2.37$ ) are very different in the two cases, but, within each case, for different values of the critical temperature, they are perfectly superimposable. The first case with  $\lambda_{13} = 6$  can be considered extreme, but, in any case, the scaling law continues to hold perfectly. Finally we have tried to study what happens in the case of extreme strong coupling when the ratio  $\frac{k_B T_c}{\Omega_0}$  is equal to one. We will study the third case ( $\nu_{13} = \nu_{23} = 1$ ). The rate  $\frac{k_B T_c}{\Omega_0} = 1$  is considered extreme strong coupling and not physical because we find, as it is shown in Figure 5,  $\lambda_{tot} \geq 20$ . For these values of the coupling constants it becomes problematic to define the value of the gap as well because the equation that defines it has more solutions [30]. Furthermore, in this regime it is probable that Migdal’s theorem no longer holds and Eliashberg’s equations become enormously more complicated. Obviously this situation has no connection with iron pnictides or any other known multiband systems.

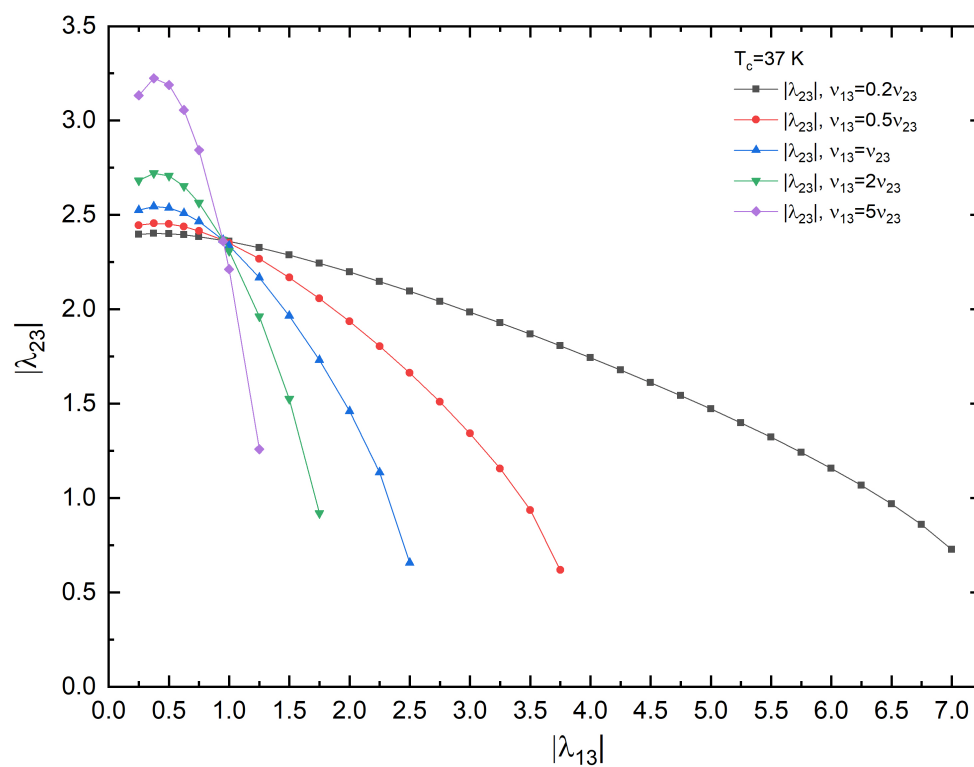


**Figure 1.** (Color online)  $|\lambda_{23}|$  versus  $|\lambda_{13}|$ .

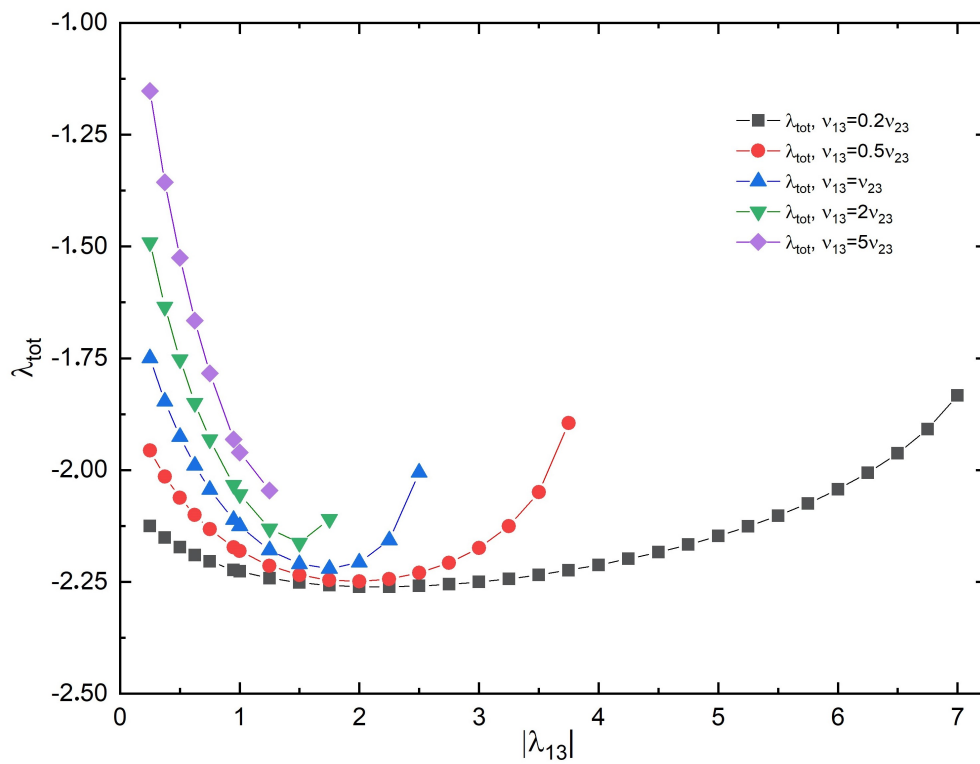


**Figure 2.** (Color online)  $\lambda_{tot}$  versus  $|\lambda_{13}|$ .

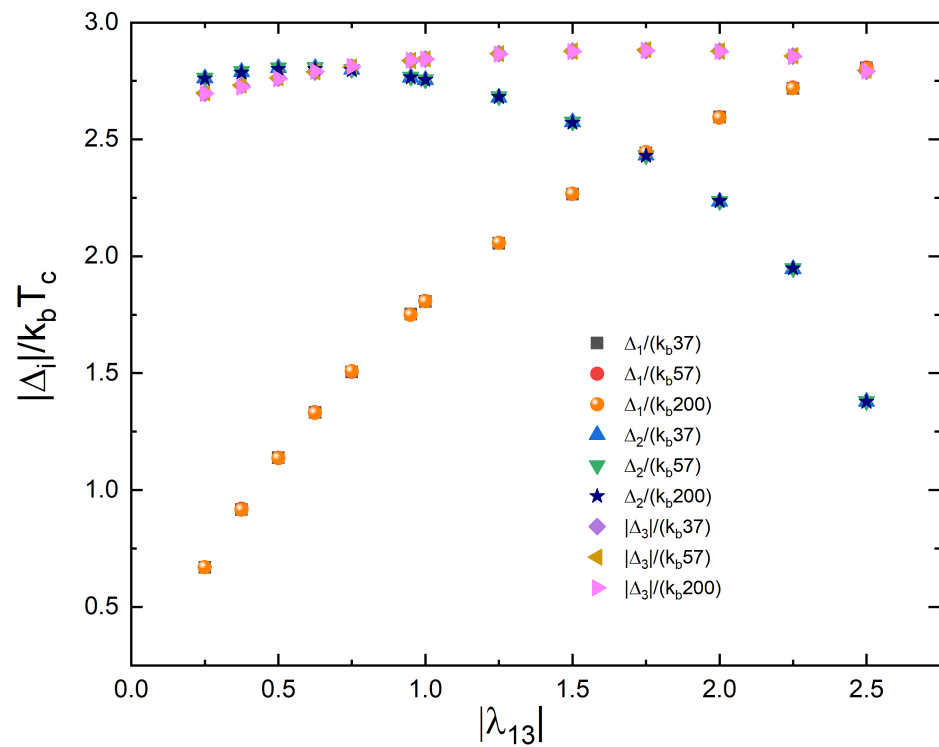


**Figure 3.** (Color online)  $|\Delta_i|/k_B T_c$  for  $T_c = 37$  K,  $T_c = 57$  K and  $T_c = 20$  K versus  $|\lambda_{13}|$  in the case where the values of the partial dots at the Fermi level ( $N_i(0)$ ) are all equals ( $\nu_{13} = \nu_{23} = 1$ ).

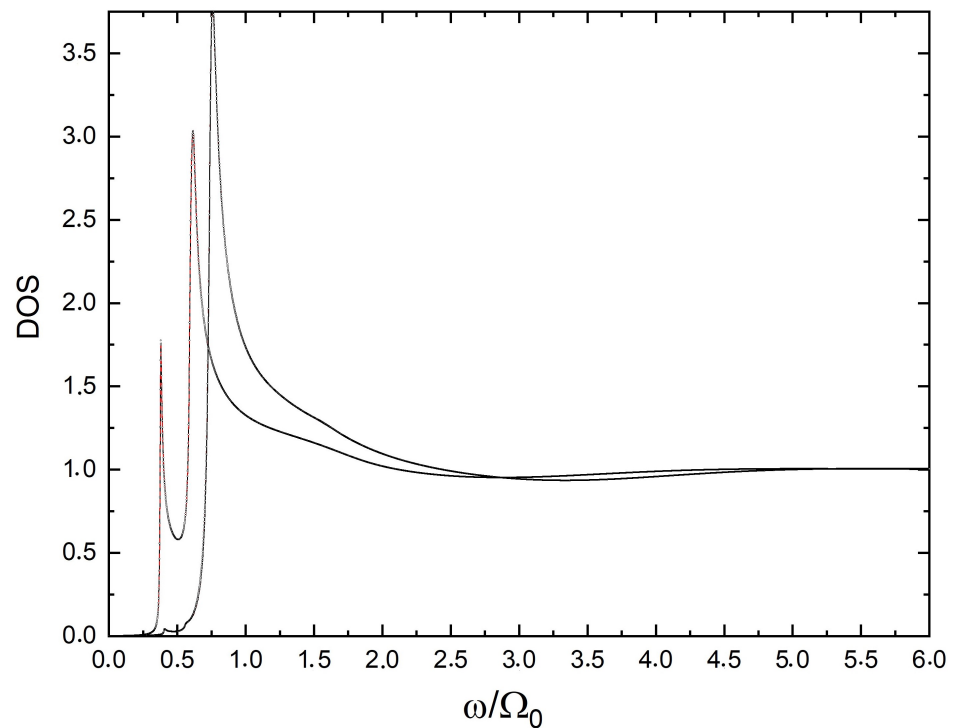


**Figure 4.** (Color online) Densities of states calculated at  $T = T_c/12$  for  $T_c = 37$  K (red line),  $T_c = 57$  K (black line) and  $T_c = 200$  K (open black circles) versus  $\omega/\Omega_0$  in the first ( $\nu_{13} = 0.2$  and  $\nu_{23} = 1$  with  $\lambda_{13} = 6.0000$  and  $\lambda_{23} = 1.1577$ ) and third cases ( $\nu_{13} = 1$  and  $\nu_{23} = 1$  with  $\lambda_{13} = 0.9500$  and  $\lambda_{23} = 2.3657$ ).

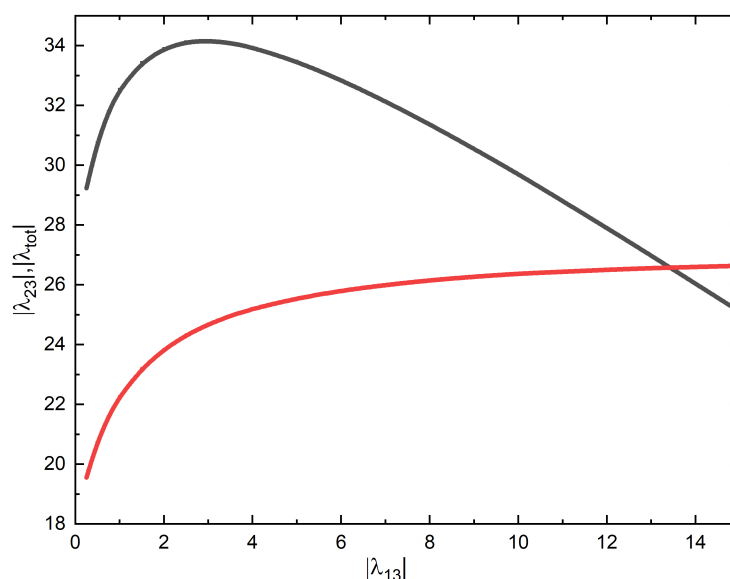


**Figure 5.** (Color online)  $\lambda_{tot}$  versus  $|\lambda_{13}|$  (solid red line) and  $\lambda_{23}$  versus  $|\lambda_{13}|$  (black solid line) in the extreme strong coupling case ( $\frac{k_B T_c}{\Omega_0} = 1$ ) when the values of the partial dos at the Fermi level ( $N_i(0)$ ) are all equals ( $\nu_{13} = \nu_{23} = 1$ ).

#### 4. Conclusions

In this article, it has been shown that the three-band model has universal aspects as the link between  $\lambda_{23}$  and  $\lambda_{13}$  or the value of  $|\Delta_i|/k_B T_c$ , which are independent of the particular features of a given system and from a particular critical temperature. These universal aspects are related to the assumption that the typical bosonic energy correlates with the critical temperature, as shown by the experimental data. By assuming  $\Omega_0 = 4.65 k_B T_c$ , a strict constraint is imposed on the value of the electron–boson coupling constant. A similar conclusion may be derived from the analysis of the Allen–Dynes formula [31] for the critical temperature in a one-band model. Here, we prove, in a fully numerical solution to the Eliashberg equation for a multi-band model, that such a constraint holds with great accuracy.

**Funding:** This research received no external funding.

**Institutional Review Board Statement:** Not applicable.

**Informed Consent Statement:** Not applicable.

**Data Availability Statement:** Not applicable.

**Acknowledgments:** G.A.U. acknowledges support from the MEPhI Academic Excellence Project (Contract No. 02.a03.21.0005).

**Conflicts of Interest:** The author declares no conflict of interest.

#### References

1. Ghigo, G.; Torsello, D.; Ummarino, G.A.; Gozzelino, L.; Tanatar, M.A.; Prozorov, R.; Canfield, P.C. Disorder-Driven Transition from  $s_{\pm}$  to  $s_{++}$  Superconducting Order Parameter in Proton Irradiated  $Ba(Fe_{1-x}Rh_x)_2As_2$  Single Crystals. *Phys. Rev. Lett.* **2018**, *121*, 107001. [CrossRef] [PubMed]
2. Torsello, D.; Ummarino, G.A.; Gozzelino, L.; Tamegai, T.; Ghigo, G. Comprehensive Eliashberg analysis of microwave conductivity and penetration depth of K-, Co-, and P-substituted  $BaFe_2As_2$ . *Phys. Rev. B* **2019**, *99*, 134518. [CrossRef]
3. Torsello, D.; Cho, K.; Joshi, K.R.; Ghimire, S.; Ummarino, G.A.; Nusran, N.M.; Tanatar, M.A.; Meier, W.R.; Xu, M.; Bud'ko, S.L.; et al. Analysis of the London penetration depth in Ni-doped  $CaKFe_4As_4$ . *Phys. Rev. B* **2019**, *100*, 094513. [CrossRef]
4. Ghigo, G.; Ummarino, G.A.; Gozzelino, L.; Gerbaldo, R.; Laviano, F.; Torsello, D.; Tamegai, T. Effects of disorder induced by heavy-ion irradiation on  $(Ba_{1-x}K_x)Fe_2As_2$  single crystals, within the three-band Eliashberg  $s_{\pm}$  wave model. *Sci. Rep.* **2017**, *7*, 13029. [CrossRef] [PubMed]



5. Torsello, D.; Ummarino, G.A.; Bekaert, J.; Gozzelino, L.; Gerbaldo, R.; Tanatar, M.A.; Canfield, P.C.; Prozorov, R.; Ghigo, G. Superconductivity of underdoped  $PrFeAs(O, F)$  investigated via point-contact spectroscopy and nuclear magnetic resonance. *Phys. Rev. B* **2020**, *13*, 064046.
6. Ummarino, G.A. Phenomenology of  $CaKFe_4As_4$  explained in the framework of four bands Eliashberg theory. *Physica C* **2016**, *529*, 50. [\[CrossRef\]](#)
7. Ummarino, G.A.; Galasso, S.; Sanna, A. A phenomenological multiband Eliashberg model for  $LiFeAs$ . *J. Phys. Condens. Matter* **2013**, *25*, 205701. [\[CrossRef\]](#) [\[PubMed\]](#)
8. Inosov, D.S.; Park, J.T.; Charnukha, A.; Li, Y.; Boris, A.V.; Keimer, B.; Hinkov, V. Crossover from weak to strong pairing in unconventional superconductors. *Phys. Rev. B* **2011**, *83*, 214520. [\[CrossRef\]](#)
9. Paglione, J.; Greene, R.L. High-temperature superconductivity in iron-based materials. *Nat. Phys.* **2010**, *6*, 645. [\[CrossRef\]](#)
10. Mazin, I.I.; Singh, D.J.; Johannes, M.D.; Du, M.H. Unconventional Superconductivity with a Sign Reversal in the Order Parameter of  $LaFeAsO_{1-x}F_x$ . *Phys. Rev. Lett.* **2008**, *101*, 057003. [\[CrossRef\]](#)
11. Mazin, I.I.; Schmalian, J. Pairing symmetry and pairing state in ferropnictides: Theoretical overview. *Physica C* **2009**, *469*, 614. [\[CrossRef\]](#)
12. Hirschfeld, P.J.; Korshunov, M.M.; Mazin, I.I. Gap symmetry and structure of Fe-based superconductors. *Rep. Prog. Phys.* **2011**, *74*, 124508. [\[CrossRef\]](#)
13. Coombes, J.M.; Carbotte, J.P. Dependence of  $2\Delta_0/k_B T_c$  on the shape of electron-phonon spectral density. *J. Low Temp. Phys.* **1986**, *63*, 431. [\[CrossRef\]](#)
14. Coombes, J.M.; Carbotte, J.P. Dependence of superconducting thermodynamics ratios on the shape of the electron-phonon spectral density. *Phys. Rev. B* **1988**, *38*, 8697. [\[CrossRef\]](#) [\[PubMed\]](#)
15. Carbotte, J.P. Properties of boson-exchange superconductors. *Rev. Mod. Phys.* **1990**, *62*, 1027. [\[CrossRef\]](#)
16. Boeri, L.; Calandra, M.; Mazin, I.I.; Dolgov, O.V.; Mauri, F. Effects of magnetism and doping on the electron-phonon coupling in  $BaFe_2As_2$ . *Phys. Rev. B* **2010**, *82*, 020506. [\[CrossRef\]](#)
17. Eliashberg, G.M. Interactions between electrons and lattice vibrations in a superconductors. *Sov. Phys. JETP* **1960**, *11*, 696.
18. Ummarino, G.A. Eliashberg Theory. In *Emergent Phenomena in Correlated Matter*; Pavarini, E., Koch, E., Schollwöck, U., Eds.; Forschungszentrum Jülich GmbH and Institute for Advanced Simulations: Jülich, Germany, 2013; pp.13.1–13.36, ISBN 978-3-89336-884-6.
19. Chubukov, A.V.; Pines, D.; Schmalian, J. *A Spin Fluctuation Model for d-Wave Superconductivity*; Bennemann, K.H., Ketterson, J.B., Eds.; Superconductivity: Novel Superconductors; Springer: Berlin/Heidelberg, Germany, 2008; Volume II.
20. Manske, D.; Eremin, I.; Bennemann, K.H. *Electronic Theory for Superconductivity in High-T<sub>c</sub> Cuprates and Sr<sub>2</sub>RuO<sub>4</sub>*; Bennemann, K.H., Ketterson, J.B., Eds.; Superconductivity: Novel Superconductors; Springer: Berlin/Heidelberg, Germany, 2008; Volume II.
21. Marsiglio, F. Eliashberg theory of the critical temperature and isotope effect. Dependence on bandwidth, band-filling, and direct Coulomb repulsion. *J. Low Temp. Phys.* **1992**, *87*, 659. [\[CrossRef\]](#)
22. Choi, H.Y. Finite bandwidth effects on the transition temperature and NMR relaxation rate of impure superconductors. *Phys. Rev. B* **1996**, *53*, 8591. [\[CrossRef\]](#)
23. Sadovskii, M.V. Antiadiabatic Phonons and Superconductivity in Eliashberg–McMillan Theory. *J. Supercond. Nov. Magn.* **2020**, *33*, 19. [\[CrossRef\]](#)
24. Ummarino, G.A.; Gonnelli, R.S.  $s$ – and  $d$ –wave solution of Eliashberg equations with finite bandwidth. *Physica C* **2000**, *341–348*, 295. [\[CrossRef\]](#)
25. Ummarino, G.A.; Tortello, M.; Daghero, D.; Gonnelli, R.S. Three-band  $s \pm$  Eliashberg theory and the superconducting gaps of iron pnictides. *Phys. Rev. B* **2009**, *80*, 172503. [\[CrossRef\]](#)
26. Ummarino, G.A.; Tortello, M.; Daghero, D.; Gonnelli, R.S. Predictions of Multiband  $s \pm$  Strong-Coupling Eliashberg Theory Compared to Experimental Data in Iron Pnictides. *J. Supercond. Nov. Magn.* **2011**, *24*, 247. [\[CrossRef\]](#)
27. Ummarino, G.A. Multiband  $s \pm$  Eliashberg theory and temperature-dependent spin-resonance energy in iron pnictide superconductors. *Phys. Rev. B* **2011**, *83*, 092508. [\[CrossRef\]](#)
28. Ummarino, G.A.; Gonnelli, R.S. Breakdown of Migdal’s theorem and intensity of electron-phonon coupling in high-T<sub>c</sub> superconductors. *Phys. Rev. B* **1997**, *56*, 14279. [\[CrossRef\]](#)
29. Inosov, D.S.; Park, J.T.; Bourges, P.; Sun, D.L.; Sidis, Y.; Schneidewind, A.; Hradil, K.; Haug, D.; Lin, C.T.; Keimer, B.; et al. Normal-state spin dynamics and temperature-dependent spin-resonance energy in optimally doped  $BaFe_{1.85}Co_{0.15}As_2$ . *Nat. Phys.* **2010**, *6*, 178. [\[CrossRef\]](#)
30. Ummarino, G.A.; Gonnelli, R.S. Real-axis direct solution of the  $d$ –wave Eliashberg equations and the tunneling density of states in optimally doped  $Bi_2Sr_2CaCu_2O_{8+x}$ . *Physica C* **1999**, *328*, 189–194. [\[CrossRef\]](#)
31. Allen, P.B.; Dynes, R.C. Transition temperature of strong-coupled superconductors reanalyzed. *Phys. Rev. B* **1975**, *12*, 905. [\[CrossRef\]](#)

**Disclaimer/Publisher’s Note:** The statements, opinions and data contained in all publications are solely those of the individual author(s) and contributor(s) and not of MDPI and/or the editor(s). MDPI and/or the editor(s) disclaim responsibility for any injury to people or property resulting from any ideas, methods, instructions or products referred to in the content.